Structure and Properties of Welded Long-Range-Ordered Alloys

Weldability of long-range-ordered alloys, a new class of high temperature material, has been found to be good

BY S. A. DAVID, D. N. BRASKI AND C. T. LIU

ABSTRACT. Sound autogenous welds can be produced readily in thin sheets of the $(Fe,Ni)_3(V,Ti)$ and $(Fe,Co)_3(V,Ti)$ long-range-ordered (LRO) alloys. Welds of $(Fe,Ni)_3(V,Ti)$ were disordered, but the tensile properties were not adversely affected. A reordering heat treatment restored the weldment properties to those of the base metal. Welds of $(Fe,Co)_3(V,Ti)$ remained ordered after the weld thermal cycle. Tensile properties similar to those of the base metal and a more uniform hardness profile can be produced by using a postweld heat treatment. In many potential applications at elevated temperatures, the use of a postweld reordering heat treatment would be unnecessary for both alloys because the weldment would reorder itself during service. Factors that seem to influence the weldment properties include ordered domain size and precipitation of carbides.

Introduction

Long-range-ordered alloys are a unique class of material with an atomic arrangement distinctly different from that of conventional or disordered alloys. Below the critical ordering temperature (T_c), alloying atoms in LRO alloys arrange themselves on specific sites and form an ordered crystal structure. Superior performance of these alloys is associated with the relatively slow atomic mobility and unique dislocation dynamics in ordered lattices. The yield strength of many LRO alloys increases rather than decreases with increasing temperature (Refs. 1-6). The alloys generally have better creep and fatigue strengths at elevated temperatures. However, their tendency to be brittle in the ordered state has limited their use for structural applications. Work by Liu, *et al.* (Refs. 7, 8), on cobalt-base ordered alloys with compositions $(Fe,Co)_3V$ has overcome this limitation. By adjusting composition and ordered crystal structure, they have been able to control the ductility of the ordered alloy. This has led to the development of ductile LRO alloys with general compositions of $(Fe,Ni)_3V$, $(Fe,Co,Ni)_3V$ and $(Fe,Co)_3V$ at the Oak Ridge National Laboratory (ORNL) for elevated-temperature structural applications (Ref. 8).

An important step in the development of these alloys is the determination of which alloys may be easily fabricated by welding. The fact that these alloys exhibit an order-disorder reaction at T_c adds a new dimension to the problems encountered in structural members subjected to weld thermal cycles. The atomic rearrangement and its kinetics could influence the properties of the weldment to a great extent. At present, there are only limited studies on characterization of weld behavior and associated phase change in ordered alloys (Ref. 9).

This paper describes some unique microstructural characteristics and tensile properties of welds in these alloys. Two LRO alloys were chosen for this study: $(Fe_{22}Co_{78})_3(V_{98}Ti_2)$, with a high T_c of 950°C (1742°F), and $(Fe_{50}Ni_{50})_3(V_{98}Ti_2)$, with a lower T_c of 670°C (1238°F). The paper delves into the order-disorder reaction response of these alloys to weld thermal cycles and the effect of postweld reordering heat treatments on the tensile properties of the welds.

Experimental Procedure

Four hundred g (14.1 oz) ingots of $(Fe,Ni)_3(V,Ti)$ and $(Fe,Co)_3(V,Ti)$ alloys were prepared by arc melting and drop casting under argon. The nominal compositions are shown in Table 1. The titanium in the alloy was added as a modifier to replace vanadium and improve the elevated temperature ductility (Ref. 8). The ingots were clad in molybdenum sheets, and they were hot rolled at 1100°C (2012°F) to a thickness of 2.5 mm (0.10 in.). The cladding was removed, and the sheet was cold rolled to a final thickness of 0.76 mm (0.03 in.). The sheet was annealed for 20 min at 1100°C and quenched in water to produce a disordered structure; subsequently, an ordering heat treatment was given. The ordering heat treatment for $(Fe,Ni)_3(V,Ti)$ alloy involved annealing the alloy for one day at 630°C (1166°F), one day at 600°C (1112°F), and two days at 550°C (1022°F). The $(Fe,Co)_3(V,Ti)$ alloy was annealed for 5 h at 800°C (1472°F), followed by 17 h at 700°C (1292°F).

Autogenous gas tungsten arc (GTA) welds were made in an inert-atmosphere welding chamber containing 75% He and 25% Ar. The welding variables used were arc voltage, 12 to 14 V; current, 40 A; and welding speed, 254 mm/min (10 in./min).

Welds were prepared for metallographic examination by standard techniques and etched with a solution consisting of 40% HNO_3, 40% H_2O and 20% HF (by volume). Microhardness traverses were made across the welds by using a Kentron microhardness tester with a 100 g load. Specimens for transmission electron microscopy (TEM) were prepared by

Table 1—Alloy Compositions

Alloy	Fe	Ni	Co	V	Ti
	Weight percent				
$(Fe,Ni)_3(V,Ti)$	37.6	39.6		22.4	0.4
$(Fe,Co)_3(V,Ti)$	16.3		61.1	22.2	0.4

Paper presented at the 64th AWS Annual Convention held in Philadelphia, Pa., April 24-29, 19B3.

S. A. DAVID, D. N. BRASKI and C. T. LIU are members of the Metals and Ceramics Division, Oak Ridge National Laboratory, Oak Ridge, Tenn.

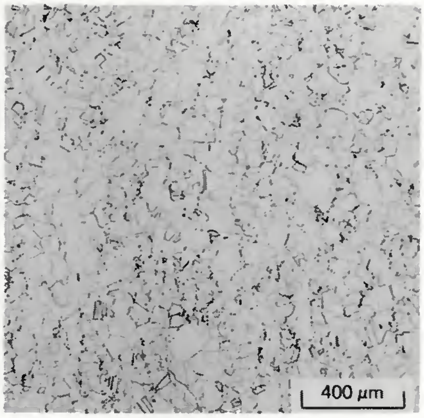

Fig. 1 — Base metal microstructure of (Fe,Ni)₃(V,Ti) long-range-ordered (LRO) alloy

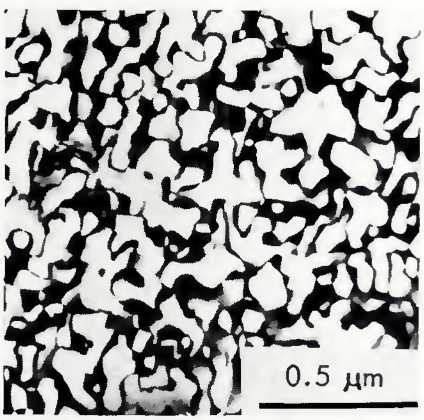

Fig. 2 — Ordered domains (light areas) and APBs (dark ribbons) in (Fe,Ni)₃(V,Ti) LRO alloy base metal. Image formed with (100) superlattice reflection

electropolishing 3 mm (0.12 in.) discs in a solution of 87.5% methanol and 12.5% H_2SO_4 (by volume) at −10°C with 15 V DC and ~100 mA current.

X-ray diffraction patterns were made with filtered Cr radiation with a 114.6 mm Debye-Scherrer camera. The lattice parameters and ordered structures were determined from needle specimens cut from the fusion region in weldments.

In order to determine the effect of ordering on mechanical properties, tensile tests were performed on a sheet specimen with a gauge section of 13 × 2 × 0.76 mm (0.51 × 0.08 × 0.03 in.). All tensile specimens were pulled at room temperature at a crosshead speed of 2.5 mm/min (0.10 in./min) in an Instron testing machine. The load-time curves were used to obtain the tensile data. Tensile properties of both welded and unwelded (Fe,Ni)₃(V,Ti), and of 2.5 mm (0.10 in.) thick sheet material were determined by using tensile specimens having a gauge section 20 mm long × 1.5 mm wide (0.79 × 0.06 in.). The GTA welds were oriented transversely through the midpoint of the gauge section. Several of the welded specimens were given the same ordering heat treatment described above to reorder the fusion and heat-affected zone (HAZ) of the weldment.

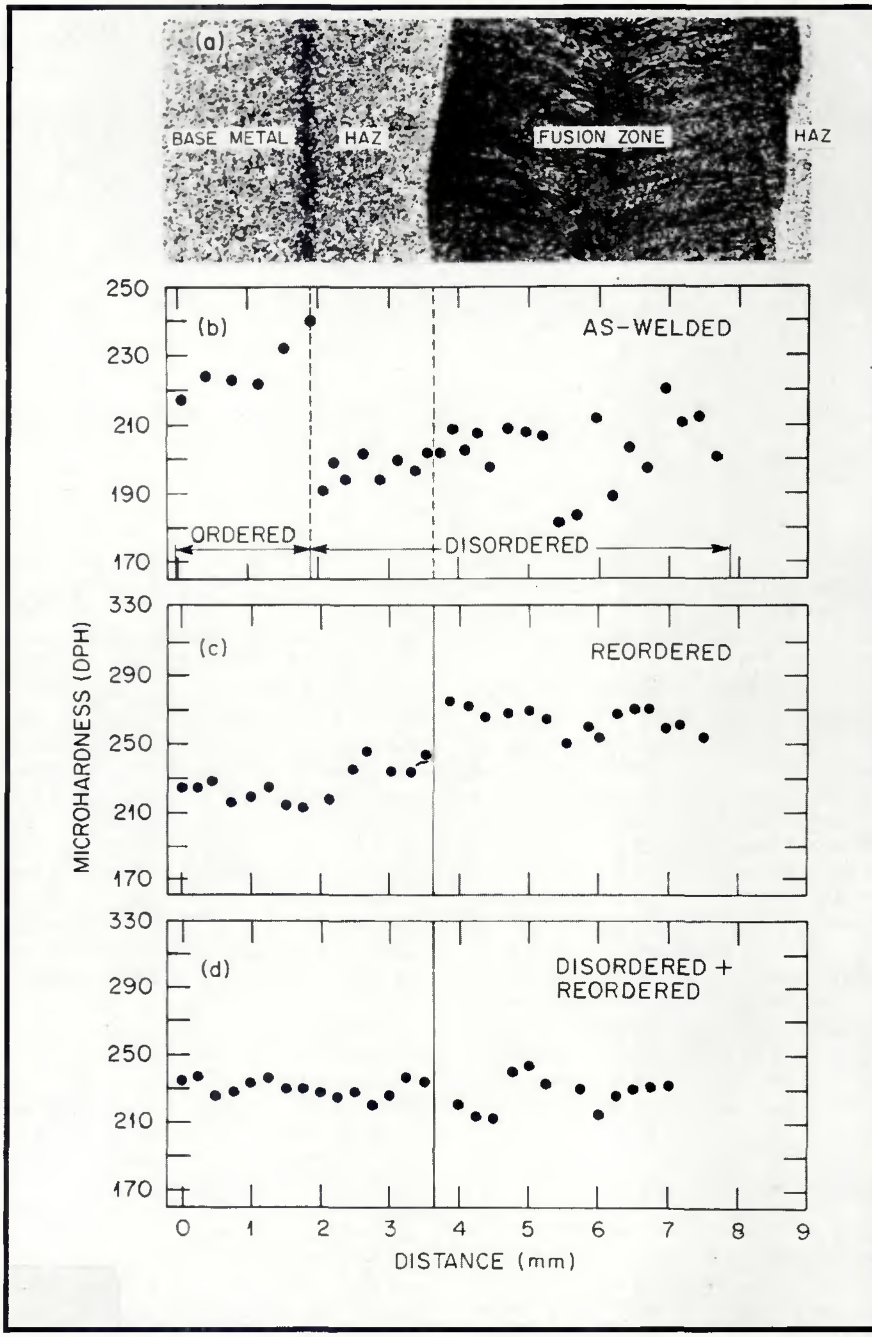

Fig. 3 — Macrograph of GTA weld of (Fe,Ni)₃(V,Ti) LRO alloy showing base metal, HAZ and fusion zone. Note narrow band between base metal (ordered) and HAZ (disordered). Also shown below are microhardness traverses across the weldment for different conditions

Results and Discussion

Structure and Properties of Welded (Fe,Ni)₃(V,Ti)

Weld Microstructure. The base metal microstructure shown in Fig. 1 contains a fine equiaxed structure with a significant number of annealing twins. The TEM analysis shows ordered domains and antiphase boundaries (APBs), as revealed in the dark field by using a superlattice reflection — Fig. 2. The light areas are ordered domains, which are separated by dark ribbons (APBs). The average domain size was measured to be 71 nm in diameter. When the alloy is in the disordered state, the ordered domains and APBs do not exist. In addition to the domain structure, TEM results revealed

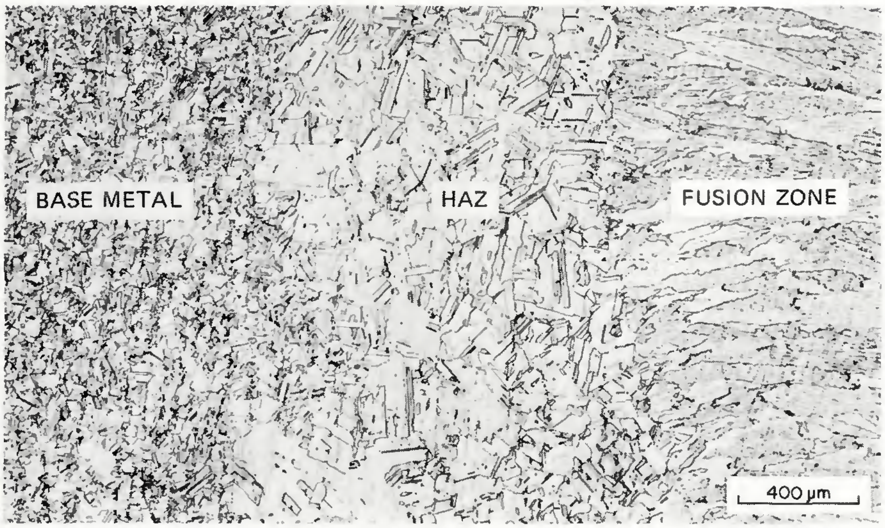

Fig. 4 — Microstructure of the (Fe,Ni)$_3$(V,Ti) LRO alloy weldment after a disordering-reordering heat treatment. Note the coarse HAZ grain structure

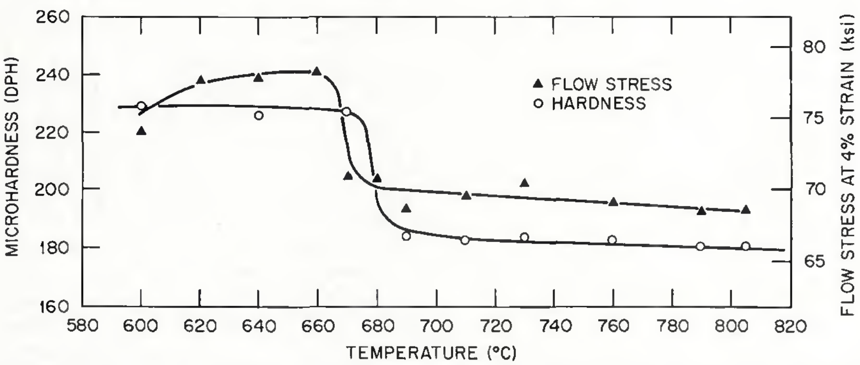

Fig. 5 — Microhardness and flow stress at 4% strain for (Fe,Ni)$_3$(V,Ti) LRO alloy as a function of temperature

the presence of small quantities of TiN, VC and unidentified Ti-rich precipitates in the matrix (Ref. 9).

The GTA welds of the alloy (Fe,Ni)$_3$(V,Ti) showed no evidence of cracking. Figure 3A is a macrograph of the weld showing three distinct regions: fusion zone, HAZ and base metal. A distinct narrow band separates the base metal from the HAZ. This band that separates the ordered structure in the base metal from the disordered HAZ will be discussed later. A microhardness traverse across the weldment is shown in Fig. 3B. The microhardness of the base metal averaged 222 DPH, dropping to 198 and 204 DPH in the HAZ and fusion zone, respectively. Another noteworthy feature is a peak hardness of 240 DPH at the diffuse boundary that separated the base metal from the HAZ. The HAZ is defined as that region of material that was heated above T_c (670°C/1238°F), but below the solidus temperature.

No significant grain coarsening due to welding was observed in the HAZ. During the weld thermal cycle, the portion of the base metal that encounters temperatures in excess of the critical ordering temperature of 670°C (1238°F) becomes disordered, and there is insufficient time during cooling from a weld thermal cycle for the structure to reorder.

The narrow band between the HAZ and the base metal has been investigated extensively (Ref. 9). While appearing to be a diffuse boundary at low magnification, it actually contains a sharp interface dividing the base metal and the HAZ. In fact, a sharp interface would define the critical temperature isotherm that the material encountered during the weld thermal cycle. No unusual microstructure was observed at this interface. The reasons for the sharp contrast in etching and the initial increase in hardness at the interface are still not clear.

The fusion zone of the weld metal consists of single-phase columnar grains with a cellular dendritic substructure — Fig. 3A. Because no superlattice lines were observed by selected area electron diffraction, the fusion zone had a disordered crystal structure rather than an ordered crystal structure. The lattice parameter in the fusion zone was measured to be 0.3597 nm. No evidence of hot cracking or any other defects was observed within the fusion zone, thus showing that the material is weldable in thin sections. The hardness of the fusion zone was comparable to that of the HAZ, but less than that of the base metal. As described before, the low hardness values are mainly due to the disordered structure within the fusion zone.

To observe the effects of a reordering heat treatment on the (Fe,Ni)$_3$(V,Ti) welds, the welds were given the same ordering treatment as performed initially. Except for the disappearance of the diffuse boundary, the reordering treatment produced very little change in the microstructure of the weldment. However, there was a remarkable increase in the hardness profile of the fusion zone and a slight increase in the hardness of the HAZ, as shown in Fig. 3C. The TEM analysis of the HAZ and of the fusion zone showed ordered domains and APBs in the HAZ and in the fusion zone. Also, the domain sizes in the reordered HAZ and fusion zone were smaller than in the base metal by more than a factor of two. This difference in domain size is attributed to the greater total time the base metal had spent at the ordering temperature. The additional increase in the hardness of the fusion zone, compared with that of the HAZ, is due to the extensive precipitation of fine VC observed on the grain boundaries, as well as on matrix dislocations (Ref. 9). No such precipitation was observed in the HAZ after reordering heat treatment.

To eliminate such variations in hardness profiles across the weldment, the weldment was given a disordering treatment at 1100°C (2012°F) for 20 min, followed by a standard ordering treatment. One of the results of such a heat treatment is some grain coarsening in the HAZ, as shown in Fig. 4. The reason for this unusual grain growth is not understood at the present time. Figure 3D shows the hardness profile across the weldment after the ordering treatment. The profile appears to be uniform across the weldment. The coarse grain structure of the HAZ and the fusion zone, as shown in Fig. 4, appears to have very little effect on the hardness. It is believed that ordering of the structure has more influence on the hardness profile than other features of the microstructure.

Mechanical Properties. In order to determine the effect of order on room temperature mechanical properties, sheet specimens of the base metal were heat treated to various temperatures below and above T_c, followed by a water quenching. Figure 5 is a plot of hardness and flow stress at 4% strain as a function of quench temperature. The plot clearly shows a sharp drop in both

Table 2—Room Temperature of Experimental LRO Alloys

Alloy	Specimen	Yield Strength (MPa)	Ultimate Tensile Strength (MPa)	Uniform Elongation (%)	Total Elongation (%)	Comments
$(Fe,Ni)_3(V,Ti)$	Base metal	379	1223	34.4	34.4	
$(Fe,Ni)_3(V,Ti)$	As-welded	483	724	24.3	26.6	Failed in fusion zone
$(Fe,Ni)_3(V,Ti)$	Welded and reordered	475	1070	26.0	26.0	Failed in fusion zone
$(Fe,Ni)_3(V,Ti)$	Welded, disordered and reordered	349	1020	30.0	30.5	Failed in fusion zone
$(Fe,Co)_3(V,Ti)$	Base metal	216	1474.5	44.4	44.4	
$(Fe,Co)_3(V,Ti)$	Welded, disordered and reordered	238	1145.0	37.8	37.8	Failed in fusion zone

hardness and flow stress at the quench temperature above 670°C (1238°F), the critical ordering temperature of the $(Fe,Ni)_3(V,Ti)$ alloy. The alloy is, thus, softer in the disordered state than in the ordered state. This result is consistent with the observation of a steep decrease in hardness between the ordered base metal and the disordered HAZ—Fig. 3B. Quantitatively, there was less drop in hardness of the HAZ and the fusion zone than in the specimens that were heated to temperatures above T_c and quenched. This may be related to one or a combination of various factors, *i.e.,* lattice strain in the HAZ and fusion zone introduced by the lattice expansion in going from the ordered to the disordered state, residual solidification shrinkage and/or thermal stresses, or possibly some additional VC precipitation in the fusion zone. Also, the TEM analysis showed an increase in the dislocation density compared with the base metal.

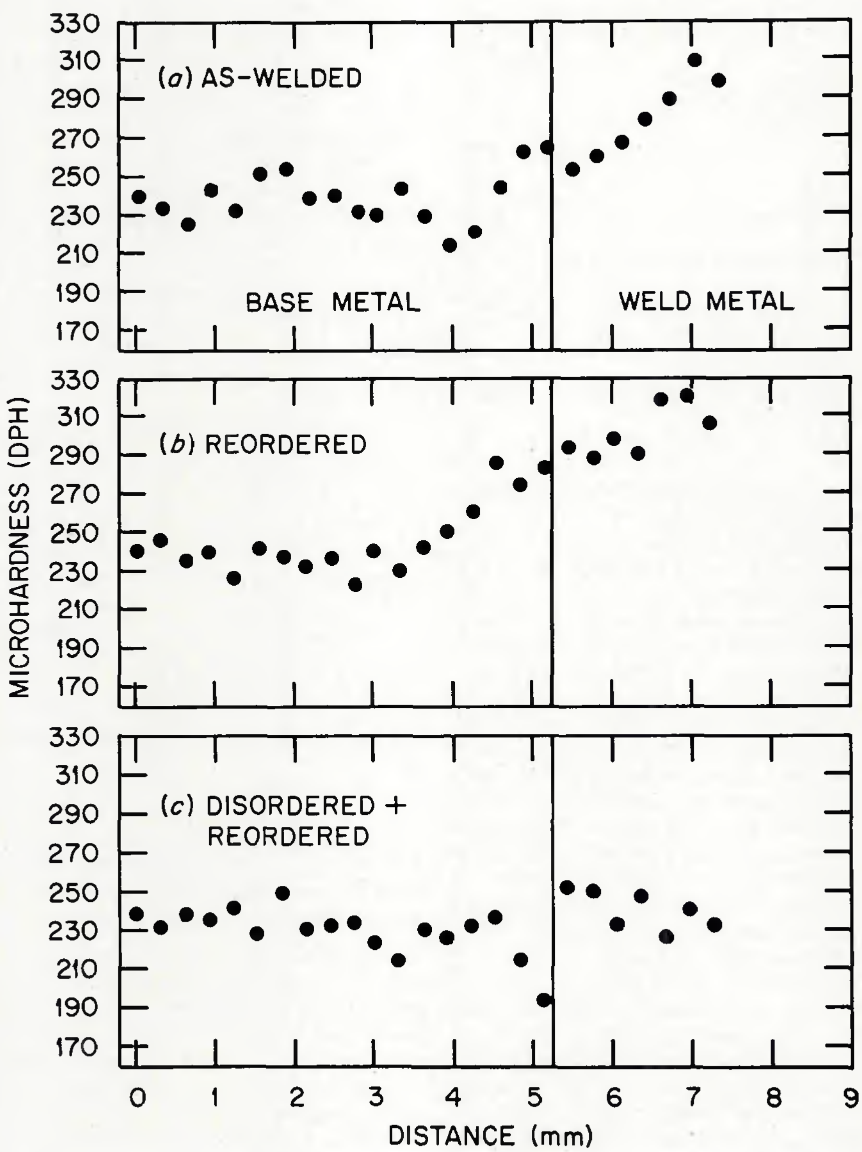

Fig. 6—Microhardness traverses across the $(Fe,Co)_3(V,Ti)$ LRO alloy weldment for different conditions

The results of tensile tests on welded and unwelded $(Fe,Ni)_3(V,Ti)$ specimens are presented in Table 2. Two specimens were tested at each condition, and the values are the average of two tests. All welded specimens failed in the fusion zone. Welding produced a measurable increase in the yield strength, but it reduced the ultimate strength because the disordered fusion zone was inherently weaker than the starting, ordered base metal. The weakened fusion zone also decreased the uniform and total elongation values by its inability to work-harden like the ordered material. Reordering below T_c increased the ultimate strength markedly but had little effect on elongation, probably because the yield strength was still ~100 MPa (14.5 ksi) above that for the ordered base metal. A complete ordering heat treatment, involving a quench from 1100°C (2012°F) and annealing below T_c, produced properties of the weld that were nearly the same as those of the base metal. From a practical standpoint, welded structures of $(Fe,Ni)_3(Ti,V)$ probably could be used in the as-welded condition as long as the structural loading was not excessive. In elevated-temperature applications, the welds would automatically reorder during the initial service period and become stronger with no losses of ductility. For most applications, a disordering heat treatment involving a quench from 1100°C (2012°F) probably would be unnecessary.

Structure and Properties of Welded $(Fe,Co)_3(V,Ti)$

Weld Microstructure. The GTA welds of the $(Fe,Co)_3(V,Ti)$ alloy were produced with no signs of cracking or any other defects. The hardness traverse across the

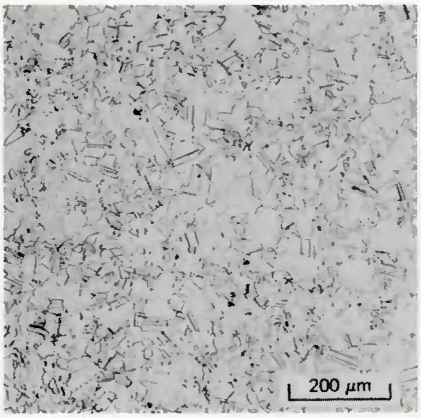

Fig. 7—Base metal microstructure of (Fe,Co)$_3$(V,Ti) LRO alloy

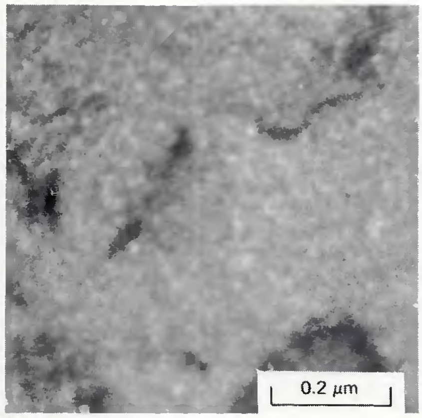

Fig. 8—Dark-field image showing small ordered domains in the fusion zone of as-welded (Fe,Co)$_3$(V,Ti) LRO alloy

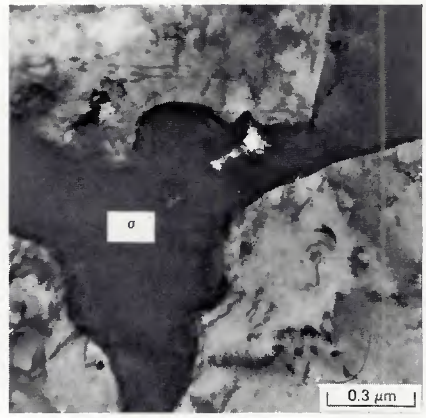

Fig. 9—Electron micrograph showing sigma phase in the fusion zone of as-welded (Fe,Co)$_3$(V,Ti) LRO alloy

weldment is shown in Fig. 6A. The macrostructure and the hardness profile were observed to be entirely different from those of the (Fe,Ni)$_3$(V,Ti) alloy discussed earlier. The HAZ with disordered structure as defined for (Fe,Ni)$_3$(V,Ti) was not present. The hardness gradually increased from an average value of 250 DPH in the base metal to 305 DPH in the fusion zone. No evidence of softening in the fusion or HAZ zones was observed.

The ordered alloy has an L1$_2$ type cubic ordered structure existing below 950°C (1742°F). Here again, titanium has been added to the alloy as a modifier to replace vanadium and improve the elevated-temperature ductility (Ref. 8). A low-magnification micrograph of the ordered (Fe,Co)$_3$(V,Ti) base metal is shown in Fig. 7. The base metal contains a fine equiaxed structure with a significant amount of annealing twins. The TEM analysis showed ordered domains and APBs, as revealed with dark-field microscopy using a superlattice reflection. No evidence of TiN or VC precipitates was found. Also, the TEM analysis revealed that both the HAZ and fusion zone were ordered, in spite of the fact that these regions experienced temperatures well above T$_c$ during welding. With the higher critical ordering temperature compared with the previous alloy and probably different ordering kinetics, the cobalt-base LRO alloy was able to retain its ordered structure after welding. Atomic order in the HAZ and in the fusion zone was also confirmed by x-ray diffraction, which showed weak superlattice lines corresponding to L1$_2$ type ordered lattice structure. The lattice parameter in the fusion zone was measured to be 0.3568 nm, which agrees well with the value obtained from the ordered state in an alloy with a similar composition.

The fusion zone of the weld metal consists of single-phase columnar grains with cellular dendritic substructure. No evidence of hot cracking or any other defects was observed. The relatively higher hardness values obtained in the fusion zone may be related to domain size. An analysis of the domain size showed that the average domain size in the fusion zone was 5 to 12 nm, while that of the base metal was 295 nm. Figure 8 is a dark-field photo showing small ordered domains in the fusion zone. Hardening attributed to antiphase domains has been observed previously by the other investigators in a number of ordered alloys, such as Cu$_3$Al (Refs. 10–12), Ni$_3$Fe (Ref. 12) and Mg$_3$Cd (Ref. 13). Generally, the hardness increased with reduction in antiphase domain size, and the peak hardness usually occurred at a domain size of 0.5 nm diameter (Ref. 6). The degree of ordering or the departure from perfect order as described by long-range-order parameter S was determined in our study by a technique described elsewhere (Ref. 14). The S was determined to be 0.95 for the base metal and 0.75 for the fusion zone. This lower value for the fusion zone is consistent with the small domain size. Also, TEM analysis revealed the presence of an Fe-V type sigma phase in the fusion zone, as shown in Fig. 9. Weak reflection lines from the tetragonal sigma phase were also detected by x-ray diffraction.

To observe the effects of reordering on the weld, the weld was given a reordering heat treatment of 5 h at 800°C (1472°F), as described earlier. The reordering treatment produced very little change in the microstructure or in the hardness profile of the weldment, as shown in Fig. 6B.

To eliminate drastic variations in hardness observed across the (Fe,Co)$_3$(V,Ti) alloy weldment, a disordering heat treatment, followed by an ordering heat treatment, was carried out on the as-welded specimen. The weldment was quenched in water from 1100°C (2012°F), followed by the ordering treatment for this alloy. Figure 6C shows a fairly uniform hardness profile across the weldment after it was given this treatment. Except for a uniform domain size across the weldment and perhaps a reduction in the residual stress, no other microstructural changes were observed in the fusion zone after the disorder-reorder heat treatment. This result suggests that domain size plays an important role in the strength of weldments. Welds of (Fe,Co)$_3$(V,Ti) with nearly the same tensile properties as those of the base metal can be produced by using the GTA process and a postweld reordering treatment, as demonstrated by the data in Table 2. The purpose of the postweld reordering treatment was not to reorder the fusion zone per se, but to increase the domain size and degree of order (S-parameter). In many elevated-temperature applications below 950°C (1742°F), such increases would occur with time anyway, and a postweld heat treatment would be unnecessary.

Conclusions

Sound welds can be produced readily in the ductile long-range-ordered alloys. However, depending on the T$_c$, the response of this class of material to weld thermal cycle varies from alloy to alloy. The HAZ and fusion zone of (Fe,Ni)$_3$(V,Ti) welds were disordered, with a decreased hardness within the HAZ and the fusion zone. The disordered weld was somewhat weaker and less ductile than the base metal. Use of a postweld reordering heat treatment restored the tensile properties of the weld to that of the unwelded base metal, but in many applications such a treatment may not be required. The HAZ and fusion zone of the (Fe,Co)$_3$(V,Ti) welds remained ordered, with increased hardness within the HAZ and the fusion zone. Tensile properties similar to those of the base metal and a more uniform hardness profile can be produced by using a postweld heat treatment. Welds in the LRO alloys appear to be stronger than the base metal when the weldment is ordered. Possible explanations for this behavior include the small size of the ordered domain in the fusion zone and/or the presence of VC precipitates in the fusion zone.

Acknowledgment

The authors gratefully acknowledge the encouragement of C. J. McHargue and J. O. Stiegler as program managers. The authors also thank M. L. Santella and J. A. Horton, Jr., for reviewing the manuscript, and M. L. Anderson and K. W. Gardner for typing it. This research was sponsored by the Division of Materials Sciences, U. S. Department of Energy, under contract DE-AC05-840R21400 with Martin Marietta Energy Systems, Inc.

References

1. Thornton, R. H., Davies, R. G., and Johnston, T. L. 1970. The temperature dependence of the flow stress of the γ' phase based upon Ni_3Al. *Metall. Trans.* 1:207.
2. Coply, S. M., and Kear, B. H. 1967. Temperature and orientation dependence of the flow stress in off-stoichiomotric Ni_3Al (γ phase). *Metall. Soc.* AIME 239:977.
3. Stoloff, N. S., and Davies, R. G. 1964. The plastic deformation of ordered FeCo and Fe_3Al alloys. *Acta. Metall.* 12:473.
4. Liang, S. J., and Pope, D. P. 1977. The yield stress of $L1_2$ ordered alloys. *Acta. Metall.* 25:485–493.
5. Lall, C., Chin, S., and Pope, D. P. 1979. The orientation and temperature dependence of the yield stress of $Ni_3(Al,Nb)$ single crystals. *Metall. Trans.* A 10A:1323.
6. Stoloff, N. S., and Davies, R. G. 1966. The mechanical properties of ordered alloys. *Prog. Mater. Sci.* 13(1):1–34.
7. Liu, C. T., and Inouye, H. 1979. Control of ordered structure and ductility of $(Fe,Co,Ni)_3V$ alloys. *Metall. Trans.* 10A:1515.
8. Liu, C. T. 1984. Physical metallurgy and mechanical properties of ductile ordered alloys $(Fe,Co,Ni)_3V$. *Inter. Met. Rev.* 29(3):168–194.
9. Braski, D. N., and David, S. A. 1983. Weld microstructure of $(Ni,Fe)_3(V,Ti)$ long-range-ordered alloys. *Met. Trans.* 14A:1785–1791.
10. Davies, R. G., and Stoloff, N. S. 1963. Order and domain hardening in Cu_3 Au type superlattice alloys. *Acta. Metall.* 11:1347.
11. Ardley, G. W. 1955. On the effect of ordering upon the strength of Cu_3Au wires. *Acta. Metall.* 3:525-532.
12. Briggs, W. D., and Broom, T. 1954. The yield strength of partly ordered Cu_3Au wires. *Phil. Mag.* 45:246-248.
13. Davies, R. G., and Stoloff, N. S. 1964. Mechanical properties and superlattice formation of Mg_3Cd. *Trans. Amer. Inst. Met. Engrs.* 230:390–395.
14. Braski, D. N., Bentley, J., and Cable, J. W. 1982. Measurement of degree of ordered alloys by convergent beam electron diffraction patterns. *40th Ann. Proc. Electron Microscopy Soc. Amer.* Washington, D. C., ed. G. W. Bailey.